Regular Article

PHYSICAL CHEMISTRY RESEARCH
Published by the
Iranian Chemical Society
www.physchemres.org
info@physchemres.org

*Phys. Chem. Res., Vol. 11, No. 1, 9-21, March 2023*
**DOI: 10.22036/PCR.2022.324549.2016**

# *In-Silico* Molecular Docking, Validation, Drug-Likeness, and ADMET Studies of Antiandrogens to Use in the Fight against SARS-CoV-2

A. Saih[a,b,*], E. Imane[a,c], H. Baba[a,b], M. Bouqdayr[a,b], H. Ghazal[d,e], S. Hamdi[f], S. Moussamih[g], H. Bennani[b], R. Saile[b], A. Kettani[b] and L. Wakrim[a]

[a]*Virology Unit, Immunovirology Laboratory, Institut Pasteur du Maroc, 20360 Casablanca, Morocco*
[b]*Laboratory of Biology and Health, URAC 34, Faculty of Sciences Ben M'Sik Hassan II University of Casablanca, Morocco*
[c]*Centre for Doctoral Studies in Health Sciences, Faculty of Medicine and Pharmacy, Casablanca, Morocco*
[d]*National Center for Scientific and Technical Research (CNRST), Rabat 10102, Morocco*
[e]*Department of Fundamental Sciences, School of Medicine, Mohammed VI University of Health Sciences, Casablanca, Morocco*
[f]*Environmental Health Laboratory, Institut Pasteur du Maroc, 20360 Casablanca, Morocco*
[g]*Immunology and Biodiversity Laboratory, Faculty of Sciences Ain Chock, Hassan II University of Casablanca, Morocco*
*(Received 14 January 2022, Accepted 29 March 2022)*

The SARS-CoV-2 is the novel coronavirus that causes the pandemic COVID-19, which has originated in Wuhan, China, in December 2019. Early studies have generally shown that human Angiotensin-Converting Enzyme 2 (ACE2) and transmembrane protease serine 2 (TMPRSS2) are responsible for the viral entry of SARS-CoV-2 into target cells. TMPRSS2 as androgen-regulated is highly expressed in the prostate and other tissues including the lung. We investigated the interaction between the TMPRSS2 protein and selected antiandrogens, namely bicalutamide, enzalutamide, apalutamide, flutamide, nilutamide, and darolutamide using *in-silico* molecular docking. The results showed that apalutamide (-8.8 Kcal $mol^{-1}$) and bicalutamide (-8.6 Kcal $mol^{-1}$) had the highest docking score. The molecular docking process was validated by re-docking the peptide-like-inhibitor-serine protease hepsin and superimposing them onto the reference complex. Last of all, the tested compounds have been evaluated for their pharmacokinetic and drug-likeness properties and concluded that these compounds except nilutamide (mutagenic) can be granted as potential inhibitors of SARS-CoV-2. This *in-silico* study result encourages its use as means for drug discovery of new COVID-19 treatment.

**Keywords:** TMPRSS2, Antiandrogens, Molecular Docking, SARS-CoV-2, ADMET

## INTRODUCTION

The current pandemic of coronavirus disease 2019 (COVID-19) is caused by the severe acute respiratory syndrome coronavirus 2 (SARS-CoV-2), with approximately, 330, 200, 901 confirmed cases, 5,561,083 deaths, and 268, 520, 410 recovered patients as of January 17, 2022 [5]. Recent studies have examined the implication of Angiotensin-Converting Enzyme 2 (ACE2) and the human transmembrane protease serine 2 (TMPRSS2) in SARS-CoV-2 infection [13,30].

TMPRSS2 is an androgen-regulated cell surface serine protease that cleaves SARS-CoV-2 spike glycoprotein in two segments called S1 and S2 mediating viral entry into the host cells. [29]. The highest expression of TMPRSS2 has been shown in the adult prostate, lung, thyroid, kidney, salivary gland, pancreas, liver, and other tissues [15].

*Corresponding author. E-mail: asmae.saih-etu@etu.univh2c.ma

TMPRSS2 protein is composed of 492 amino acid residues (AA), with three domains, namely N-terminal LDL-receptor class A (LDLPR) (113-148), scavenger receptor cysteine-rich called (SRCR) domain (193-246), and a C-terminal domain that includes the active site of TMPRSS2 known also as the catalytic triad (His296, Asp345, and Ser441) [23].

As previously mentioned by Squire *et al.* (2011), TMPRSS2 plays a direct role in prostate cancer progression [28]. The study by Afar *et al.* (2001) found that androgen treatment led to a diminution in TMPRSS2 expression [33]. Another study by Ragia *et al.*, (2020) showed that antiandrogens such as Enzalutamide, Apalutamide, and Darolutamide would tend to a reduction in TMPRSS2 expression provoking a less entry of SARS-CoV-2 into host cells and consequently reducing the severity of COVID-19 [24].

The current report sheds a light on the interaction between the generated model of TMPRSS2 and selected antiandrogens inhibitors, namely bicalutamide, enzalutamide, apalutamide, flutamide, nilutamide, and darolutamide using a molecular docking approach.

## MATERIAL AND METHODS

### Model Building and Protein Preparation for Docking

The TMPRSS2 amino acids sequence was obtained from The Universal Protein Resource (Uniprot) database (www.uniprot.org) (Uniprot ID: O15393) [32]. The TMPRSS2 3D structure was predicted using the Swiss-Model server [35]. For this study, we used the crystal structure of the extracellular region of the transmembrane serine protease hepsin with the covalently bound preferred substrate (PDB ID: 1z8g.1, resolution = 1.55 Å) as a template. Subsequently, the predicted model was carried out to determine a refined model by using the ModRefiner server [36]. The predicted model was validated and evaluated by PROCHECK, and Verify3D tools, respectively [17,10].

AutoDock software, an automated package of protein-ligand docking, which has two versions; AutoDock 4 and AutoDock vina [21], was used for TMPRSS2 preparation: before docking, the refined protein was initiated by adding hydrogens atoms followed by the addition of Kollman charges and then saved in Protein Data Bank (PDB) format [3].

### Ligand Preparation

The chemical structures of the inhibitors bicalutamide, enzalutamide, apalutamide, flutamide, nilutamide, and darolutamide were obtained from the PubChem database [34] in Spatial Data File (SDF) format and converted to PDB format using Discovery Studio [7]. Then, the structures were carried out in the MarvinSketch (ChemAxon) [18], and optimized for energy minimization using MMFF94 (Merck Molecular Force Field 94) force field [11] Structures of all the ligands were loaded to AutoDock software.

### Molecular Docking

The docking simulations between the aforementioned six inhibitors and TMPRSS2 were processed using the AutoDock vina program, with the Lamarckian Genetic Algorithm (LGA). Then, a grid box of 60x60x60 points was constructed targeting the entire active site of TMPRSS2 (His 296, Thr 341, Asn 343, and Asp 345), where the grid center was at X = 26.728, Y = 1.637, Z = 15.739, and the dimensions of the grid box were size x = 36, size_y = 36, size_z = 36, with grid spacing of 0.6 Å and exhaustiveness = 8. Docking simulations were performed with an initial population size of 150 to generate 50 conformations with a medium number of evaluations equal to 2,500,000. Other docking parameters such as rate of gene mutation and rate of the crossover were set as default, and all AutoDock vina [31] output files were analyzed by the PyMol program [37] and Discovery studio [7] to generate 2D and 3D protein-ligand interactions.

### Binding-pocket Analysis of TMPRSS2

The predicted-binding pocket of *TMPRSS2* protein was carried out using the Computed Atlas of Surface Topography of proteins (CASTp) server [1]. An online web server was used to identify pockets located on protein structure.

### Docking Validation Process

The peptide-like inhibitor from the serine protease

hepsin was removed and re-docked using AutoDock software [31]. Later, by using PyMol [37], the re-docked complex was superimposed onto the reference ligand and the root mean square deviation (RMSD) was determined in order to ensure that the re-docked peptide-like inhibitor bind to the active site with low deviation value to the reference ligand.

### ADMET and Drug Likeness Prediction

Pharmacokinetic properties are critical in identifying drug molecule oral bioavailability, cell permeation, metabolism, and excretion. The ADMET and *in-silico* pharmacokinetic parameters of the six tested molecules were carried out using Swissadmet and PkCSM web servers [6,23].

## RESULTS AND DISCUSSION

This study aimed to investigate the existing compounds from PubChem that may potentially interact with the TMPRSS2 protein, and consequently be used for SARS-CoV-2 treatment. The TMPRSS2 protein used in this study was obtained in its 3D structure from the Research Collaboratory for Structural Bioinformatics database (RCSB-PDB) [3]. Physicochemical properties of the selected TMPRSS2 inhibitors were retrieved from the PubChem website [34] (Table 1).

The 3D structure of TMPRSS2 protein was performed by Swiss-Model using the crystal structure of the extracellular region of the transmembrane serine protease hepsin with the covalently bound preferred substrate as a template (Fig. 1A). The generated structure was validated using PROCHECK and Verify 3D. Ramachandran plot showed that the generated structure has 90.4% of its residues in the most favored regions (Fig. 1B) [14]. Additionally, the generated model was assessed by using Verify 3D and 93.68% of its residues have averaged 3D-1D > 0.2 (Fig. 1C).

The TMPRSS2 protein was docked with the six ligands, namely the aforementioned inhibitors: Bicalutamide, enzalutamide, apalutamide, flutamide, nilutamide, and darolutamide, with AutoDock vina software generating the same grid box dimensions, which helped to understand the binding affinity of these inhibitors. Binding affinities of the selected six ligands are presented in Table 7 within the range of -7.3 (flutamide and darolutamide), -7.6 (enzalutamide and nilutamide), -8.6 (bicalutamide), and -8.8 (apalutamide) Kcal $mol^{-1}$ (Supplementary Table 1 and Fig. 2).

As a result, Apalutamide presented the best binding affinity score (-8.8 Kcal $mol^{-1}$). The AutoDock Vina docked complex showed that the residues Arg 147, Leu 151, and Cys 241 participated in hydrogen bond interactions with apalutamide. Bicalutamide had the second-best docking score (-8.6 Kcal $mol^{-1}$). We found that the four TMPRSS2 residues Arg 150, Leu 151, Cys 241, and Asn 450 were involved in hydrogen bond interactions with bicalutamide. Enzalutamide and nilutamide have the third-best binding affinity score (-7.6 Kcal $mol^{-1}$). The AutoDock Vina docked complexes (TMPRSS2-enzalutamide), (TMPRSS2-nilutamide) were analyzed. We found that the six TMPRSS2 residues Asn 249, Ser 250, Ser 254, Gly 258 Ala

**Table 1.** Physicochemical Properties of TMPRSS2 Inhibitors from the PubChem Database [34]

| Physicochemical properties | Ligands | | | | | |
|---|---|---|---|---|---|---|
| | Bicalutamide | Enzalutamide | Apalutamide | Flutamide | Nilutamide | Darolutamide |
| PubChem CID | 2375 | 15952529 | 24872560 | 3397 | 4493 | 67171867 |
| Molecular formula | $C_{18}H_{14}F_4N_2O_4S$ | $C_{21}H_{16}F_4N_4O_2S$ | $C_{21}H_{15}F_4N_5O_2S$ | $C_{11}H_{11}F_3N_2O_3$ | $C_{12}H_{10}F_3N_3O_4$ | $C_{19}H_{19}ClN_6O_2$ |
| Molecular weight (g $mol^{-1}$) | 430.4 | 464.4 | 477.4 | 276.1 | 317.22 | 398.8 |
| Hydrogen bond donor count | 2 | 1 | 1 | 1 | 1 | 3 |
| Hydrogen bond acceptor count | 9 | 8 | 9 | 6 | 7 | 5 |
| Rotatable bond count | 5 | 3 | 3 | 2 | 1 | 6 |
| X log P3-AA | 2.3 | 3.6 | 3 | 3.3 | 2 | 1.8 |

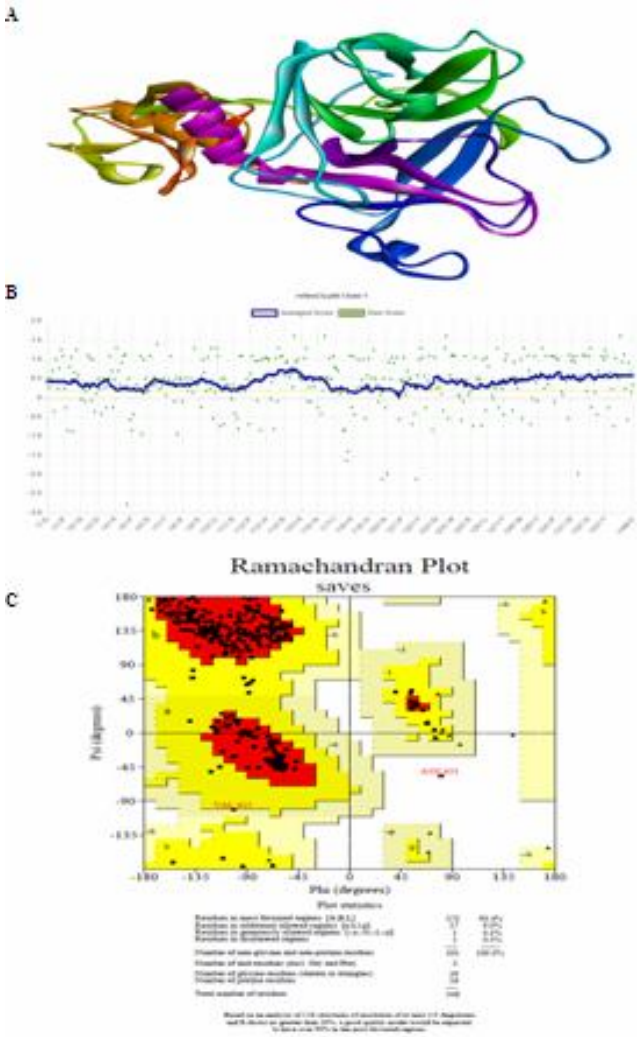


**Fig. 1.** A: Three-dimensional structure of the predicted model of TMPRSS2 using Swiss-Model. B: Verify 3D validation of the TMPRSS2 predicted model. C: PROCHECK validation of the TMPRSS2 predicted model

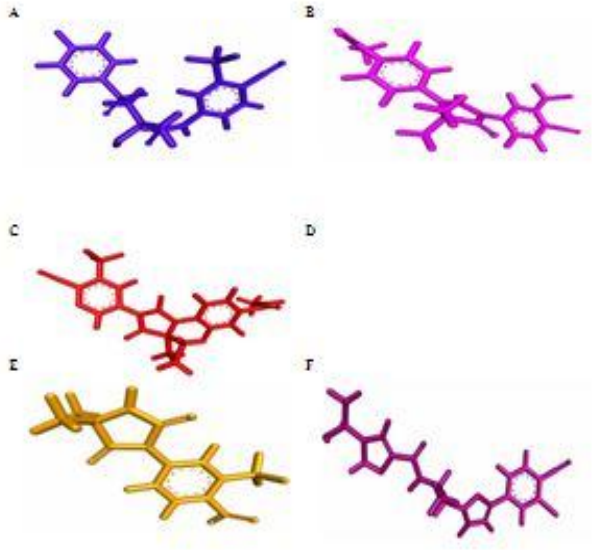


**Fig. 2.** Three-dimensional structure of selected TMPRSS2 inhibitors: A: Bicalutamide (Blue), B: Enzalutamide (Magenta), C: Apalutamide (Red), D: Flutamide (Violet), E: Nilutamide (Orange), and F: Darolutamide (Purple).

266, and Trp 267 were participated in hydrogen bond interactions with Enzalutamide, while the residues Arg 147, Arg 150, Tyr 190, and Asn 450 were involved in hydrogen bond interactions with nilutamide. Flutamide and darolutamide presented the fourth-best binding affinity score (-7.3 Kcal $mol^{-1}$). We showed that the two TMPRSS2 residues Arg 147, and Leu 151 were involved in hydrogen bonding interactions with flutamide, while the three residues Arg 182, Lys 191, and Met 488 have participated in hydrogen bonding interactions with Darolutamide (Tables 2, 3, 4, 5, 6, 7 and Fig. 3).

For targeting the active site of TMPRSS2 protein in docking studies, the CASTp server was used and identified Arg147, Val149, Arg182, Met188, and Trp454, Asp144, Glu145, and Asn146 residues, which can fit into the pockets 1 and 2 with a solvent accessible volume equal to 226.012 $Å^2$ and 179.930 $Å^2$, respectively. In general, the molecular docking analysis showed that apalutamide, flutamide, and nilutamide have different interactions with Arg147, Val149, Met188, and Trp454 in the same binding pocket of *TMPRSS2*. Supplementary Table 2 and figures 4A, 4B, and 4C show CASTp server analysis results.

Bicalutamide, also known as Casodex, is an androgen antagonist used in the prostate cancer treatment, which can block the synthesis of endogenous androgens like testosterone [2]. Bicalutamide may also reduce the severity of COVID-19 by minimizing viral replication and it has been reported to improve the clinical outcome [26]. A phase III clinical trial of Bicalutamide activity against TMPRSS2 is ongoing at the University of Florida (FL, USA), which began on October 26, 2020, and is estimated to

**Table 2.** Nonbonding Interactions of Bicalutamide Inhibitor with TMPRSS2

| Interacting residues | Distance (Å) | Bond category | Bond type |
|---|---|---|---|
| ARG 147 | 4.32 | Hydrophobic | Pi-Alkyl |
| ARG 150 | 2.43 | Hydrogen bond | Conventional hydrogen bond |
| | 2.04 | Hydrogen bond | Conventional hydrogen bond |
| | 5.38 | Hydrophobic | Pi-Alkyl |
| LEU 151 | 2.24 | Hydrogen bond | Conventional hydrogen bond |
| | 4.37 | Hydrophobic | Alkyl |
| TYR 190 | 4.44 | Hydrophobic | Pi-Alkyl |
| CYS 241 | 2.86 | Hydrogen bond | Conventional hydrogen bond |
| | 4.07 | Hydrophobic | Alkyl |
| ASN 450 | 2.41 | Hydrogen bond | Conventional hydrogen bond |

**Table 3.** Nonbonding Interactions of Enzalutamide Inhibitor with TMPRSS2

| Interacting residues | Distance (Å) | Bond category | Bond type |
|---|---|---|---|
| ASN 247 | 3.03 | Halogen | Fluorine |
| ASN 249 | 2.95 | Hydrogen bond | Conventional hydrogen bond |
| | 4.51 | Hydrophobic | Amide-Pi-Stacked |
| SER 250 | 3.38 | Hydrogen bond | Conventional hydrogen bond |
| SER 254 | 2.44 | Hydrogen bond | Conventional hydrogen bond |
| SER 256 | 4.36 | Hydrophobic | Alkyl |
| | 4.46 | Hydrophobic | Pi-Alkyl |
| GLY 258 | 3.76 | Hydrogen bond | C |
| TRP 262 | 4.09 | Hydrophobic | Alkyl |
| ALA 266 | 5.36 | Hydrophobic | Pi-Alkyl |
| | 4.47 | Hydrophobic | Alkyl |
| TRP 267 | 2.52 | Hydrogen bond | Conventional hydrogen bond |
| | 2.62 | Hydrogen bond | Conventional hydrogen bond |
| | 4.94 | Hydrophobic | Pi-Alkyl |

**Table 4.** Nonbonding Interactions of Apalutamide Inhibitor with TMPRSS2

| Interacting residues | Distance (Å) | Bond category | Bond type |
|---|---|---|---|
| ARG 147 | 2.09 | Hydrogen bond | Conventional hydrogen bond |
| | 4.23 | Hydrophobic | Alkyl |
| LEU 151 | 2.38 | Hydrogen bond | Conventional hydrogen bond |
| MET 188 | 3.34 | Halogen | Fluorine |
| CYS 241 | 2.99 | Hydrogen bond | Conventional hydrogen bond |
| ALA 243 | 5.43 | Hydrophobic | Pi-Alkyl |
| ILE 452 | 5.01 | Hydrophobic | Alkyl |
| TRP 454 | 4.90 | Hydrophobic | Pi-Alkyl |

**Table 5.** Nonbonding Interactions of Flutamide Inhibitor with TMPRSS2

| Interacting residues | Distance (Å) | Bond category | Bond type |
|---|---|---|---|
| ARG 147 | 2.33 | Hydrogen bond | Conventional hydrogen bond |
| | 3.93 | Hydrophobic | Alkyl |
| VAL 149 | 3.13 | Halogen | Fluorine |
| ARG 150 | 4.24 | Hydrophobic | Pi-Alkyl |
| LEU 151 | 2.39 | Hydrogen bond | Conventional hydrogen bond |
| MET 188 | 5.37 | Hydrophobic | Pi-Alkyl |
| | 4.62 | Hydrophobic | Alkyl |
| | 2.97 | Halogen | Fluorine |
| | 3.24 | Halogen | Fluorine |
| TYR 190 | 5.41 | Hydrophobic | Pi-Alkyl |

**Table 6.** Nonbonding Interactions of Nilutamide Inhibitor with TMPRSS2

| Interacting residues | Distance (Å) | Bond category | Bond type |
|---|---|---|---|
| ARG 147 | 2.11 | Hydrogen bond | Conventional hydrogen bond |
| | 4.00 | Hydrophobic | Alkyl |
| VAL 149 | 3.13 | Halogen | fluorine |
| ARG 150 | 4.67 | Electrostatic | Pi-cation |
| | 2.13 | Hydrogen bond | Conventional hydrogen bond |
| | 2.91 | Hydrogen bond | Conventional hydrogen bond |
| GLY 153 | 2.32 | Unfavorable | Acceptor/donor clash |
| MET 188 | 4.81 | hydrophobic | Alkyl |
| | 3.12 | Halogen | fluorine |
| TYR 190 | 2.61 | Hydrogen bond | Conventional hydrogen bond |
| ASN 450 | 2.56 | Hydrogen bond | Conventional hydrogen bond |
| ILE 452 | 3.83 | Hydrophobic | Pi-sigma |

**Table 7.** Nonbonding Interactions of Darolutamide Inhibitor with TMPRSS2

| Interacting residues | Distance (Å) | Bond category | Bond type |
|---|---|---|---|
| ARG 182 | 2.61 | Hydrogen bond | Conventional hydrogen bond |
| | 2.88 | Hydrogen bond | Conventional hydrogen bond |
| LYS 191 | 3.62 | Electrostatic | Pi-cation |
| | 2.84 | Hydrogen bond | Conventional hydrogen bond |
| PRO 288 | 4.43 | Hydrophobic | Alkyl |
| | 5.43 | Hydrophobic | Pi-Alkyl |
| PRO 354 | 4.78 | Hydrophobic | Alkyl |
| MET 488 | 3.49 | Hydrogen bond | C |
| | 3.68 | Hydrogen bond | C |

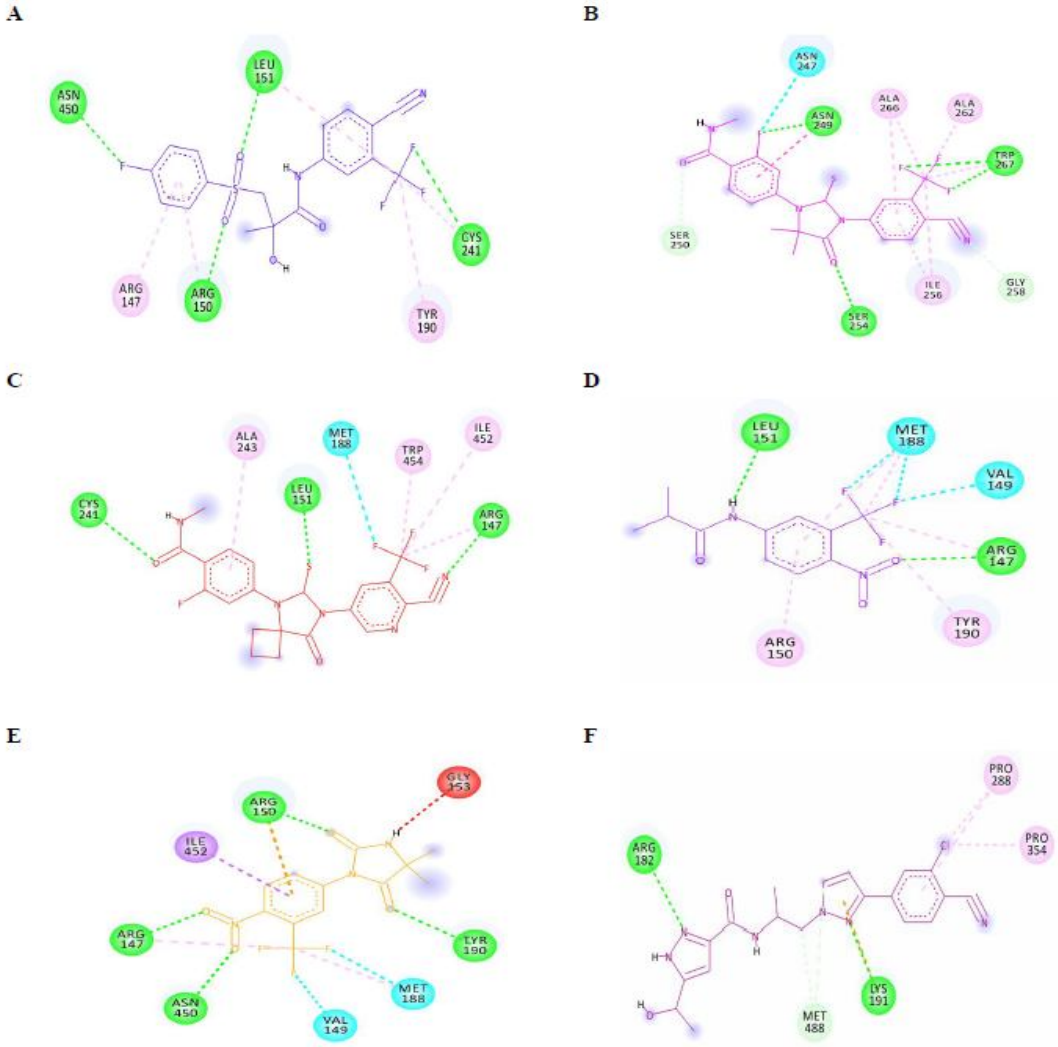


**Fig. 3.** 2D interaction diagram for selected ligands with TMPRSS2

A: Bicalutamide, B: Enzalutamide, C: Apalutamide, D: Flutamide, E: Nilutamide, and F: Darolutamide.

For targeting the active site of TMPRSS2 protein in docking studies, the CASTp server was used and identified Arg147, Val149, Arg182, Met188, and Trp454, Asp144, Glu145, and Asn146 residues, which can fit into the pockets 1 and 2 with a solvent accessible volume equal to 226.012 $Å^2$ and 179.930 $Å^2$ respectively. In general, the molecular docking analysis showed that Apalutamide, Flutamide, and Nilutamide have different interactions with Arg147, Val149, Met188, and Trp454 in the same binding pocket of TMPRSS2. Supplementary Table 2 and figures 4A, 4B, and 4C show CASTp server analysis results.

be completed by September 2022 (https://clinicaltrials.gov//(NCT 04509999)) [8]. Bicalutamide exhibited three hydrogen bond interactions with the AA residues Arg 150 (2.43 Å, 2.04 Å), Leu 151 (2.24 Å), Cys 241 (2.86 Å), and Asn 450 (2.41 Å), three Pi-Alkyl bonds with Arg 147 (4.32 Å), Arg 150 (5.38 Å), Tyr 190 (4.44 Å) and two Alkyl bonds with Leu 151 (4.37 Å), and Cys 241 (4.07 Å) in the binding site of TMPRSS2 (Fig. 3, Fig. 5A, and Table 2).

Enzalutamide or Xandi, an antiandrogen, is known to treat Metastatic Castration-Resistant Prostate Cancer (CRPC) [26]. It has been recently reported that

antiandrogens like enzalutamide reduce the severity of COVID-19 by inhibiting the expression of TMPRSS2. A phase II clinical trial of enzalutamide inhibition activity against TMPRSS2 was initiated in Sweden on July 19, 2020, and is estimated to be complete by May 2022, with the objective to be used to decrease the morbidity of COVID-19 patients (https://clinicaltrials.gov//(NCT04475601). [8]. As shown in Fig. 3, Fig. 5B, and Table 3 enzalutamide formed six hydrogen bonds with Asn 249 (2.95 Å), Ser 250 (3.38 Å), Ser 254 (2.44 Å), Gly 258 (3.76 Å), and Trp 267 (2.52 Å, 2.62 Å), two Pi-Alkyl bonds with Ser 256 (4.46 Å), Ala 266 (5.36 Å), three Alkyl bonds with Ser 256 (4.36 Å), Trp 262 (4.09 Å), and Ala 266 (4.47 Å), and Amide-Pi-Stacked with Asn 249 (4.51 Å) in the binding site of the TMPRSS2.

Apalutamide or Erleada, an androgen, was used for the treatment of Metastatic Castration-Sensitive Prostate Cancer (mCSPC) [25]. The study by D. Stroppe *et al*. (2020) found that Apalutamide may downregulate TMPRSS2 expression in prostate cancer and also against SARS-CoV-2 infection [30]. Apalutamide made three hydrogen bonds with Arg 147 (2.09 Å), Leu 151 (2.38 Å), Cys 241 (2.99 Å), two Alkyl bonds with Arg 147 (4.23 Å), Ile 452 (5.01 Å), and two Pi-Alkyl bonds with Ala 243 (5.43 Å), and Trp 454 (4.50 Å) in the binding site of the TMPRSS2 (Fig. 3, Fig. 5C, and Table 4).

Flutamide, a nonsteroidal androgen antagonist is used in the management of metastatic prostate cancer is approved for the treatment of prostate cancer. [16] Flutamide can inhibit angiotensin II receptor type II provoking natriuresis, antigrowth, vasorelaxation, and anti-inflammatory effects leading to a decrease of susceptibility to SARS-CoV-2 infection due to lower expression of ACE2 [4]. Additionally, TMPRSS2 showed reduced activity by the use of androgen receptor inhibitors such as Flutamide [20]. Flutamide set up two hydrogen bond interactions with Arg 147 (2.33 Å), and Leu 151 (2.39 Å), two Alkyl bonds with Arg 147 (3.93 Å), and Met 188 (4.62 Å), and two Pi-Alkyl bonds with Met 188 (5.37 Å), and Tyr 190 (5.37 Å) in the binding site of TMPRSS2 (Fig. 3, Fig. 5D and Table 5). Nilutamide, an androgen receptor inhibitor, is used for the treatment of stage D2 prostate cancer [9]. Importantly, this inhibitor has been recently documented to have an important role in COVID-19 treatment as a potent androgen antagonist [8]. Nilutamide engaged five hydrogen bonding interactions with Arg 147 (2.11 Å), Arg 150 (2.13 Å, 2.91 Å), Tyr 190 (2.61 Å), and Asn 450 (2.56 Å), two Alkyl bonds with Arg 147 (4.00 Å), and Met 188 (4.81 Å), Pi-Sigma bond with Ile 452 (3.83 Å), and Pi-cation bond with Arg 150 (4.67 Å) in the binding site of the TMPRSS2 (Figure 3, Figure 5E and Table 6).

Darolutamide, an antiandrogen, was used for the treatment of non-metastatic Castration-Resistant Prostate Cancer (nmCSPC) [12]. A recent study reported that Darolutamide may potentially downregulate TMPRSS2 expression and therefore reduce the severity and progression of COVID-19 [8]. Darolutamide formed five hydrogen bonds with Arg 182 (2.61 Å, 2.88 Å), Lys 191 (2.84 Å), and Met 488 (3.49 Å, 3.68 Å), two Alkyl bonds with Pro 288 (4.43 Å), and Pro 354 (4.78 Å), Pi-Alkyl with Pro 288 (5.43 Å), and Pi-cation with Lys 191 (3.62 Å) (Fig. 3, Fig. 5F and Table 7).

A re-docking of the co-crystallized ligand was performed to validate the molecular docking efficiencies. The superimposition between the re-docked co-crystallized ligand and the reference ligand using PyMol software. The figure reveals that the peptide-like AR7 is bound to the active site with a binding energy of -6.0 Kcal $mol^{-1}$. The interacting amino acid residues in the active site pocket are Leu187, His203, Pro206, Asn209, Pro245, Pro249, Asn254, Gln350, and Ser353, and a total of five hydrogen bonds were established with a threshold distance of 3.00 Å. The co-crystallized ligand (peptide-like/inhibitor) allows for a variety of interactions with TMPRSS2, including Alkyl interactions with Leu187, Pro206, Pro245, and Pro249 amino acid residues. The peptide-like also forms five H-bond interactions with His203, Asn254, Gln350, Ser353 amino acid residues. Similarly, the inhibitor interacts with Cys204 amino acid residue through carbon H-bond interaction (Fig. 6).

The re-docked co-crystallized ligand was then superimposed onto the reference ligand and an RMSD of 0.979 Å was shown.

The six tested ligands obeyed pharmacokinetic and Lipinski's properties were studied and recorded in tables. In the study, the targeted compounds were evaluated for drug-likeness based on Ghose, Veber, Egan, and Muegge filters. Drug bicalutamide, enzalutamide, apalutamide, flutamide,

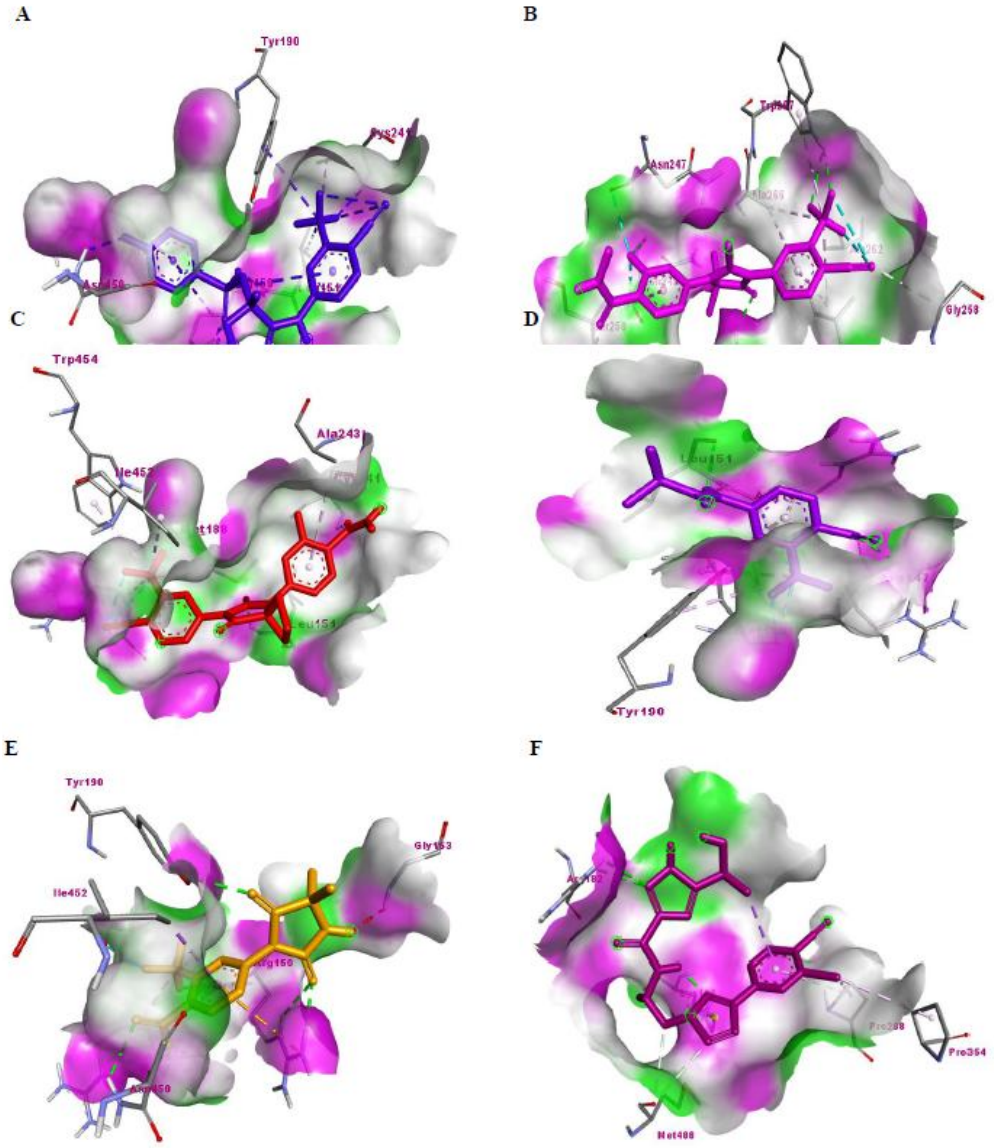


**Fig. 5.** Visualization of hydrogen bonds of TMPRSS2 with selected ligands: A: Hydrogen bonds formed by bicalutamide with TMPRSS2 residues ARG 150, LEU 151, CYS 241, and ASN 450. B: Hydrogen bonds formed by enzalutamide with TMPRSS2 residues ASN 249, SER 250, SER 254, GLY 258, and TRP 267. C: Hydrogen bonds formed by apalutamide with TMPRSS2 residues ARG 147, LEU 151, and CYS 241. D: Hydrogen bonds formed by flutamide with TMPRSS2 residues ARG 182, LYS 191, and MET 488. E: Hydrogen bonds formed by nilutamide with TMPRSS2 residues ARG 147, ARG 150, TYR 190, and ASN 450. F: Hydrogen bonds formed by darolutamide with TMPRSS2 residues ARG 182, LYS 191, and MET 488.

nilutamide, and darolutamide satisfied all the Lipinski properties. All molecules have MW <500 Da, suggesting that they could readily cross cell membranes, logP < 5, implying that they must be soluble in both lipid and aqueous solutions, H-Bond donor <5, H-Bond acceptor <10, and MR <130) (Table 8). Then, these tested compounds with bioavailability score of 0.55 are approved and satisfied all the filters (Supplementary Table 3). In terms of absorption,

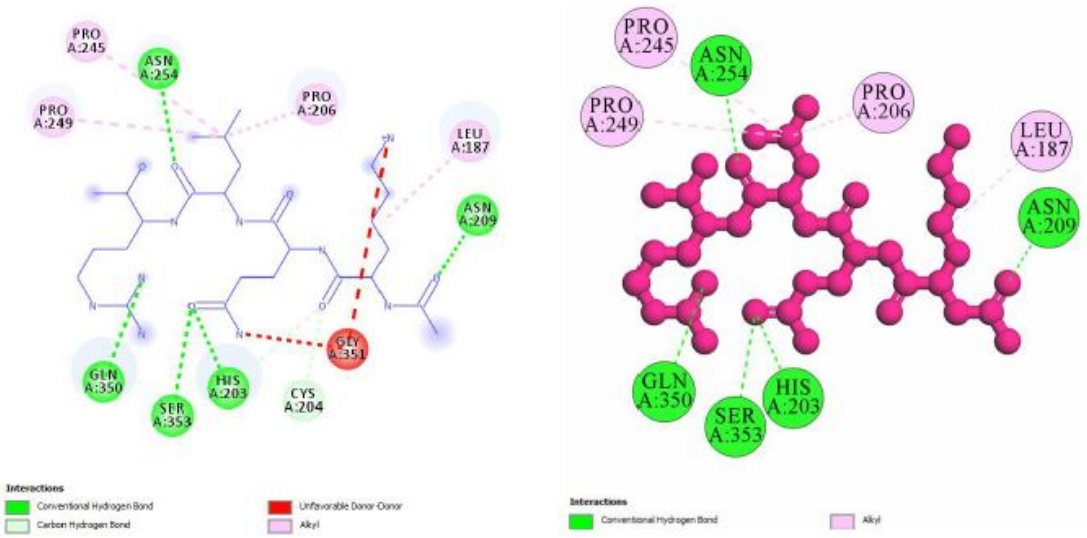


**Fig. 6.** 2D molecular interaction for the re-docked peptide-like inhibitor (co-crystallized ligand) and TMPRSS2 protein.

**Table 8.** Lipinski Results of the Six Studied Compounds

| S. No | Compounds | Properties | | | | | | Lipinski violations (<1) |
|---|---|---|---|---|---|---|---|---|
| | | Molecular weight g $mol^{-1}$ (<500) | Rotatable bonds (<10) | TPSA (Å) | logP (<5) | H-Bond acceptor (<10) | H-Bond donor (<5) | |
| 1 | Bicalutamide | 430.37 | 7 | 115.64 | 1.95 | 9 | 2 | 0 |
| 2 | Enzalutamide | 464.44 | 5 | 108.53 | 2.92 | 7 | 1 | 0 |
| 3 | Apalutamide | 477.43 | 5 | 118.94 | 2.69 | 8 | 1 | 0 |
| 4 | Flutamide | 276.21 | 5 | 74.92 | 1.85 | 6 | 1 | 0 |
| 5 | Nilutamide | 317.22 | 3 | 95.23 | 1.86 | 7 | 1 | 0 |
| 6 | Darolutamide | 398.85 | 7 | 119.62 | 1.86 | 5 | 3 | 0 |

all the targeted molecules were shown to have highly gastrointestinal absorption with intestinal absorbance value greater than 30%. The blood-brain barrier (BBB) is both a static anatomic and a dynamic barrier with active influx and efflux proteins transporters, which the most crucial are glycoprotein-P (P-gp) [27]. Compounds that reach the central nervous system (CNS) are designated as BBB+, while molecules with limited CNS are identified as BBB- [27]. Except for bicalutamide and flutamide, none of the compounds were able to cross the blood-brain barrier (BBB). A molecule with logBB > -1 is thought to be highly distributed to the brain, while a molecule with logBB < -1 is defined to be poorly distributed to the brain. As a result, except for flutamide and nilutamide, none of the compounds were able to cross the blood-brain barrier (BBB). In terms of toxicity, a negative Ames test indicates that the tested molecules are not toxic, except nilutamide which is mutagenic and, as a result, may act as a carcinogen. All molecules have synthetic accessibility values of around 3, indicating that they are simple to synthesize. Furthermore, the other pharmacokinetic properties like clearance and metabolism are approved (Supplementary Table 4).

Based on our *in-silico* study, apalutamide and bicalutamide presented both the highest binding energies of -8.8 Kcal $mol^{-1}$ and -8.6 Kcal $mol^{-1}$, respectively. These potent inhibitors for TMPRSS2 are promising candidates to

be explored for use against SARS-CoV-2 infection. It is revealed that apalutamide has a higher docking score of -8.8 Kcal $mol^{-1}$ than bicalutamide (-8.6 Kcal $mol^{-1}$), enzalutamide (-7.6 Kcal $mol^{-1}$), flutamide (-7.3 Kcal $mol^{-1}$), nilutamide (-7.6 Kcal $mol^{-1}$), and darolutamide (-7.3 Kcal $mol^{-1}$), suggesting that apalutamide is identified as the most active toward all the ligands for TMPRSS2, and may be beneficial in COVID-19 treatment.

The current study was carried out for six TMPRSS2 activity inhibitors. As these ligands engage the active site of the protease TMPRSS2 protease, therefore, inhibition of this protein is important for blocking infection by SARS-CoV-2 [19]. Bicalutamide, enzalutamide, apalutamide, flutamide, nilutamide, and darolutamide were identified to be good inhibitors for TMPRSS2 protein, but apalutamide and bicalutamide were found to have the strongest binding affinity to TMPRSS2. These results suggest the interactions of bicalutamide, enzalutamide, apalutamide, flutamide, and darolutamide may protect against severe COVID-19 and consequently reduce the severity of their complications.

## CONCLUSIONS

The six compounds tested in this study, namely bicalutamide, enzalutamide, apalutamide, flutamide, nilutamide, and darolutamide, are promising candidates for the development of new drugs against COVID-19. The selected molecules were tested as inhibitors of the TMPRSS2 protein using *in-silico* molecular docking analyses. Molecular docking results demonstrated that apalutamide and bicalutamide showed the best binding affinity against TMPRSS2. The compounds enzalutamide, flutamide, nilutamide, and darolutamide also showed a good docking score. Pharmacokinetics and toxicity parameters of the tested compounds were studied and the result showed that they have good pharmacokinetic properties, acceptable absorption, good metabolism, transformation, and are not toxic except nilutamide (mutagenic), indicating that they can be used as dependable SARS-CoV-2 potential inhibitors. Furthermore, these candidate compounds are identified as potent inhibitors for the TMPRSS2 protein of SARS-CoV-2 and as such will be suitable for experimental verification to treat COVID-19 disease. More researches are needed to investigate the relationship between the tested ligands and interaction with the TMPRSS2 protein in vivo and in vitro to confirm their inhibition activity of the TMPRSS2 protein and the clinical impact of the SARS-CoV-2 infection and COVID-19 disease.

## ACKNOWLEDGMENTS

The authors are thankful to the Pasteur Institute of Morocco for providing encouragement and facilities and resources.

## SUPPLEMENTARY MATERIALS

Supplementary Table 1: Molecular docking scores (in -Kcal $mol^{-1}$) of TMPRSS2 protein with its selected inhibitors (ligands).
Supplementary Table 2: Identification of the active site of TMPRSS2 protein using the CASTp server
Supplementary Table 3: Drug likeness results of the six studied ligands.
Supplementary Table 4: pharmacokinetic parameters of the six tested compounds.

## REFERENCES

[1] Binkowski, T. A.; Naghibzadeh, S.; Liang, J., CASTp: Computed atlas of surface topography of proteins. *Nucleic Acids Res.* **2003**, *31*, 3352-3355, DOI: 10.1093/nar/gkg512.

[2] Bohl, C. E.; Gao, W.; Miller, D. D.; Bell, C. E.; Dalton, JT.; Structural basis for antagonism and resistance of bicalutamide in prostate cancer. *Proc. Natl. Acad. Sci. U S A.* **2005**, *102*, 6201-6206, DOI: 10.1073/pnas.050038110.

[3] Burley, S. K.; Berman, H. M.; Bhikadiya, C., RCSB protein data Bank: biological macromolecular structures enabling research and education in fundamental biology, biomedicine, biotechnology and energy. *Nucleic Acids Res.* **2019**, *47*, D464-D474, DOI: 10.1093/nar/gky1004.

[4] Cava, C.; Bertoli, G.; Castiglioni, I., *In silico* discovery of candidate drugs against covid-19. *Viruses*. **2020**, *12*, 404, DOI: 10.3390/v12040404.

[5] https://www.worldometers.info/coronavirus. «COVID

Live Update: 330,200,901 Cases and 5,561,083 Deaths from the Coronavirus- Worldometer». s. d. Consulté le 17 Janvier 2022.

[6] Diana, A.; Michielin, O.; Zoete, V., SwissADME: a free web tool to evaluate pharmacokinetics, drug-likeness and medicinal chemistry friendliness of small molecules. *Sci. Rep*. **2017**, *7*, 42717, DOI: 10.1038/srep42717.

[7] Kemmish, H.; Fasnacht, M.; Yan, L., Fully automated antibody structure prediction using BIOVIA tools: Validation study. *PLoS One*. **2017**, *12*, e0177923, DOI: 10.1371/journal.pone.0177923.

[8] Depfenhart, M.; de Villiers, D.; Lemperle, G.; Meyer, M.; Di Somma, S., Potential new treatment strategies for COVID-19: is there a role for bromhexine as add-on therapy? *Intern. Emerg. Med*. **2020**, *15*, 801-812, DOI: 10.1007/s11739-020-02383-3.

[9] Desai, A.; Stadler, W. M.; Vogelzang, N. J., Nilutamide: possible utility as a second-line hormonal agent. *Urology*. **2001**, *58*, 1016-1020, DOI: 10.1016/s0090-4295(01)01455-8.

[10] Eisenberg, D.; Lüthy, R.; Bowie, J. U., VERIFY3D: assessment of protein models with three-dimensional profiles. *Methods Enzymol.* **1997**, *277*, 396-404, DOI: 10.1016/s0076-6879(97)77022-8.

[11] Ertl, P., Molecular structure input on the web. *J. Cheminform*. **2010**, *2*, 1, DOI: 10.1186/1758-2946-2-1.

[12] Fizazi, K.; Shore, N.; Tammela, T. L., Nonmetastatic, castration-resistant prostate cancer and survival with darolutamide. *N Engl. J. Med.* **2020**, *383*, 1040-1049, DOI: 10.1056/NEJMoa2001342.

[13] Hoffmann, M.; Kleine-Weber, H.; Schroeder, S., SARS-CoV-2 cell entry depends on ACE2 and TMPRSS2 and is blocked by a clinically proven protease inhibitor. *Cell.* **2020**, *181*, 271-280, DOI: 10.1016/j.cell.2020.02.052.

[14] Hollingsworth, S. A.; Karplus, P. A., A fresh look at the Ramachandran plot and the occurrence of standard structures in proteins. *Biomol. Concepts*. **2010**, *1*, 271-283, DOI: 10.1515/BMC.2010.022.

[15] Hussain, M.; Jabeen, N.; Amanullah, A., Molecular docking between human TMPRSS2 and SARS-CoV-2 spike protein: conformation and intermolecular interactions. *AIMS Microbiol.* **2020**, *6*, 350-360, DOI: 10.3934/microbiol.2020021.

[16] Goldspiel, B. R.; Kohler, D. R., Flutamide: an antiandrogen for advanced prostate cancer. *DICP.* **1990**, *24*, 616-623, DOI: 10.1177/106002809002400612.

[17] Laskowski, R. A.; M.W. Macarthur, D.S.; J. M. Thornton.; PROCHECK: A program to check the stereochemical quality of protein structures. *J. App. Crystallography.* **1993**, *26*, 283-91, DOI: 10.1107/S0021889892009944.

[18] MarvinSketch. http://www.chemaxon.com/marvin/sketch/index.jsp.

[19] McKee, D. L.; Sternberg, A.; Stange, U.; Laufer, S.; Naujokat, C., Candidate drugs against SARS-CoV-2 and COVID-19. *Pharmacol. Res.* **2020**, *157*, 104859, DOI: 10.1016/j.phrs.2020.104859.

[20] Montopoli, M.; Zumerle, S.; Vettor, R., Androgen-deprivation therapies for prostate cancer and risk of infection by SARS-CoV-2: a population-based study (N = 4532). *Ann. Oncol.* **2020**, *31*, 1040-1045, DOI: 10.1016/j.annonc.2020.04.479.

[21] Morris, G. M.; Huey, R.; Lindstrom, W., AutoDock4 and AutoDockTools4: Automated docking with selective receptor flexibility. *J. Comput. Chem.* **2009**, *30*, 2785-2791, DOI: 10.1002/jcc.21256.

[22] Pires, D. E. V.; Blundell, T. L.; Ascher, D. B., pkCSM: Predicting small-molecule pharmacokinetic and toxicity properties using graph-based signatures. *J. Med. Chem.* **2015**, *58*, 4066-4072, DOI: 10.1021/ACS.JMEDCHEM.5B00104.

[23] Piva, F.; Sabanovic, B.; Cecati, M.; Giulietti, M., Expression and co-expression analyses of TMPRSS2, a key element in COVID-19. *Eur. J. Clin. Microbiol. Infect. Dis.* **2021**, *40*, 451-455, DOI: 10.1007/s10096-020-04089-y.

[24] Ragia, G.; Manolopoulos, V. G., Inhibition of SARS-CoV-2 entry through the ACE2/TMPRSS2 pathway: a promising approach for uncovering early COVID-19 drug therapies. *Eur. J. Clin. Pharmacol.* **2020**, *76*, 1623-1630, DOI: 10.1007/s00228-020-02963-4.

[25] Sanchez, L. R.; Cathelineau, X.; Pinto, A. M. A., Clinical and surgical assistance in prostate cancer during the COVID-19 pandemic: Implementation of

assistance protocols. *Int. Braz. J. Urol.* **2020**, *46* (suppl.1), 50-61, DOI: 10.1590/S1677-5538.IBJU. 2020.S106.

[26] Scott, L. J.; Enzalutamide: A review in castration-resistant prostate cancer. *Drugs*. **2018**, *78*, 1913-1924, DOI: 10.1007/s40265-018-1029-9.

[27] Anna. W. Sobanska.; Hekner, Adam.; Brzezińska, Elżbieta.; RP-18 HPLC analysis of drugs' ability to cross the blood-brain barrier. *J. Chem.* **2019**, 1-12, DOI: 10.1155/2019/5795402.

[28] Squire, J. A.; Park, P. C.; Yoshimoto, M., Prostate cancer as a model system for genetic diversity in tumors. *Adv. Cancer Res.* **2011**, *112*, 183-216, DOI: 10.1016/B978-0-12-387688-1.00007-7.

[29] Strope, J. D.; PharmD, CHC.; Figg, W. D., TMPRSS2: Potential biomarker for COVID-19 outcomes. *J. Clin. Pharmacol.* **2020**, *60*, 801-807, DOI: 10.1002/jcph.1641.

[30] Teli, D. M.; Shah, M. B.; Chhabria, M. T., *In silico* screening of natural compounds as potential inhibitors of SARS-CoV-2 main protease and spike RBD: Targets for COVID-19. *Front. Mol. Biosci.* **2021**, *7*, 599079, DOI: 10.3389/fmolb.2020.599079.

[31] Trott, O.; Olson, A. J., AutoDock Vina: improving the speed and accuracy of docking with a new scoring function, efficient optimization, and multithread ding. *J. Comput. Chem.* **2010**, *31*, 455-46, DOI: 10.1002/ jcc.21334.

[32] UniProt, Consortium.; UniProt: a worldwide hub of protein knowledge. *Nucleic Acids Res.* **2019**, *47*, D506-D515, DOI: :10.1093/nar/gky1049.

[33] Wambier, C. G.; Goren, A.; Vaño-Galván, S., Androgen sensitivity gateway to COVID-19 disease severity. *Drug Dev Res.* **2020**, *81*, 771-776, DOI: 10.1002/ddr.21688.

[34] Wang, Y.; Xiao, J.; Suzek, T. O.; Zhang, J.; Wang, J.; Bryant, S. H., PubChem: a public information system for analyzing bioactivities of small molecules. *Nucleic Acids Res.* **2009**, *37*, W623-W633, DOI: 10.1093/nar/gkp456.

[35] Waterhouse, A.; Bertoni, M.; Bienert, S., SWISS-MODEL: homology modelling of protein structures and complexes. *Nucleic Acids Res.* **2018**, *46*, W296-W303, DOI: 10.1093/nar/gky427.

[36] Xu, D.; Zhang, Y., Improving the physical realism and structural accuracy of protein models by a two-step atomic-level energy minimization. *Biophys. J.* **2011**, *101*, 2525-2534, DOI: 10.1016/ j.bpj.2011.10.024.

[37] Yuan, Shuguang.; H. C. Stephen Chan.; Zhenquan, Hu.; Using PyMOL as a platform for computational drug design. *WIREs Comput. Mol. Sci.* **2017**, *7*, e1298, DOI: 10.1002/wcms.1298.